

Fig. 2. Model for calculating the output noise of a general linear circuit: each noise source contributes according to its particular transfer function.

The overall output spectral density will be

$$V_{on}(f) = [|H_1(j2\pi f)|^2 e_1^2 + |H_2(j2\pi f)|^2 e_2^2 + |H_3(j2\pi f)|^2 e_s^2 + |H_4(j2\pi f)|^2 e_n^2 + |H_5(j2\pi f)|^2 i_{n1}^2]^{1/2} \quad (11)$$

Equation (8) is also the transfer function for the signal. From (8) we can calculate the high-pass frequency. For the particular case when $R_s \ll R_1 + R_2$, $R_1 = R_2 = R$ and $C_1 = C_2 = C$, we have

$$\omega_m \approx \frac{(10^{1/2} - 3)^{1/2}}{RC} \approx \frac{0.4}{RC} \quad (12)$$

Equations (6) and (7) suggest that the higher the value for R_1 and R_2 as compared to R_s , the lower their contribution will be to the output noise. Furthermore, from (1) and (2) we see that the thermal noise for any resistor increases only as the square root of its ohmic value. However, from (6) and (7) we see that, from a given frequency up, the modulus of the transfer function decreases in direct proportion to the increase in the ohmic value of resistors R_1 and R_2 respectively. Given that the larger the values for R_1 and R_2 the larger the low-frequency input impedance for the amplifier, which is highly convenient, we conclude that large resistors are advisable in the circuit in Fig. 1.

There are, of course, some limits to be considered for R_1 and R_2 . Besides their lower quality, high-value resistors are susceptible to capacitive interference and, worse still, result in high noise contribution caused by the op-amp current noise ((10) and (11)). However, all of these factors can be controlled, for example, by electrical shielding and by choosing an op-amp with low noise current. Only the thermal noise associated with resistors is unavoidable; but, (6) and (7) show that the output noise caused by the thermal noise does indeed decrease when we use resistors that are large as compared to R_s .

We propose the simple model in Fig. 2 for the analysis of the noise behavior of the circuit in Fig. 1, or any other circuit which has several internal noise sources. The point is that each noise source g_i (voltage or current) has a corresponding transfer function, and those transfer functions are not all the same as the transfer function for the signal. Indeed, in our case only the thermal noise for the source resistance R_s has the same transfer function $H_3(s)$ as the signal. Therefore, we cannot directly infer any conclusions for the output noise when resistor values are chosen so that they produce specific changes, either in the signal transfer function or input impedance. Rather, the corresponding transfer functions must be considered.

TABLE I
EQUIVALENT INPUT NOISE VOLTAGE (nV, rms) FOR THE DIFFERENT NOISE SOURCES IN FIG. 1 AND FOR DIFFERENT VALUES FOR RESISTORS AND CAPACITORS

	v_1	v_2	v_3	v_4	v_5	v_6
$R_1 = R_2 = 3.3 \text{ M}\Omega$ $C_1 = C_2 = 1 \text{ }\mu\text{F}$ $R_s = 1 \text{ k}\Omega$ $R_n = 1 \text{ M}\Omega$	16	0.9	91	294	0.1	308
	1583	4.9	2876	383	8.9	3310
$R_1 = R_2 = 10 \text{ M}\Omega$ $C_1 = C_2 = 1 \text{ }\mu\text{F}$ $R_s = 1 \text{ k}\Omega$ $R_n = 1 \text{ M}\Omega$	9	0.2	91	294	0.09	308
	909	0.9	2876	323	8.9	3030
$R_1 = R_2 = 3.3 \text{ M}\Omega$ $C_1 = C_2 = 22 \text{ nF}$ $R_s = 1 \text{ k}\Omega$ $R_n = 1 \text{ M}\Omega$	401	260	91	329	3.5	587
	1619	251	2876	388	9.5	3330
$R_1 = R_2 = 10 \text{ M}\Omega$ $C_1 = C_2 = 22 \text{ nF}$ $R_s = 1 \text{ k}\Omega$ $R_n = 1 \text{ M}\Omega$	340	173	91	319	4.7	505
	967	168	2878	342	10	3060

v_1, v_2, v_3, v_4 , and v_5 , are, respectively, the rms equivalent input noise voltages due to R, R_1, R_2, R_s, v_n , and i_{n1} . v_6 is the total equivalent input noise. The op-amp was an OPA111BM and $T = 300\text{K}$.

In order to calculate the output noise for different component values in Fig. 1, we have developed a user-friendly software program based on MathCad. When $R_1 = R_2 = 3.3 \text{ M}\Omega$, $C_1 = C_2 = 1 \text{ }\mu\text{f}$, and the op-amp was an OPA111BM ($e_{nw} = 6.9 \text{ nV}/\sqrt{\text{Hz}}$, $f_{ce} = 190 \text{ Hz}$, $i_{nw} = 0.4 \text{ fA}/\sqrt{\text{Hz}}$, $f_{ci} = 0.1 \text{ Hz}$ assumed; the manufacturer specifies a flat current noise spectral density from 0.1 Hz to 20 kHz). The signal bandwidth (-3 dB) was from 0.02 Hz to 500 Hz. The 0.02 Hz high-pass frequency was determined by the amplifier; the 500 Hz low-pass frequency was assumed to be determined by a posterior filter.

The bandwidth for calculating the output noise is somewhat arbitrary. Equations (6) to (8) show that even though the band pass for the noise is determined by the components R_1, R_2, C_1 , and C_2 that also determine the signal bandwidth, the transfer functions for signal and noise are different. (It is worth noting that we are not interested in the so-called "equivalent noise bandwidth," derived from the signal bandwidth, because we consider our noise sources to be internal. Therefore they cannot be directly substituted by an equivalent constant source applied to the signal input). If we assume that a posterior filter determines the 500 Hz low-pass frequency for the signal, it is reasonable to take the same low-pass frequency for the noise.

The high-pass frequency for the noise is somewhat controversial. We propose a value dependent on the application for this frequency: low-frequency noise will influence the intelligibility of the signal only if it is perceived by the person or machine that analyzes the signal, in order to retrieve the information. Given that we were interested in the visual analysis on a cathode ray tube screen of a cyclostationary signal (the electrocardiogram, ECG), whose fundamental frequency was around 1 Hz, we considered that noise whose frequency was lower than 0.5 Hz would not affect the analysis because the human observer would not perceive it when only a short time record is displayed.

The bandwidth for calculating the output noise was, thus, 0.5 to 500 Hz. For $T = 300 \text{ K}$, $R_s = 1 \text{ k}\Omega$ and $R_n = 1 \text{ M}\Omega$, we obtained the first group of results in Table I, where v_1, v_2, v_3, v_4 , and v_5 , are, respectively, the rms equivalent

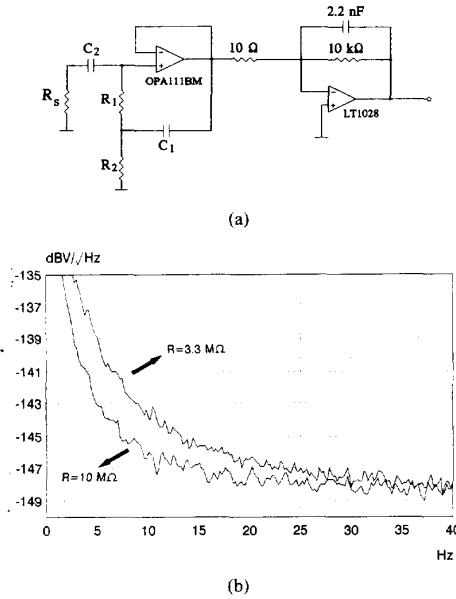


Fig. 3. (a) Experimental circuit to test the results in Table I. (b) Output noise for the circuit in Fig. 1 for $R_1 = R_2 = R = 10 \text{ M}\Omega$ and $R_1 = R_2 = R = 3.3 \text{ M}\Omega$.

input noise voltages caused by R_1 , R_2 , R_s , v_n , and i_{n1} . The total equivalent input noise is v_t .

Next, we changed R_1 and R_2 to $10 \text{ M}\Omega$ and calculated the equivalent input noise voltages from the same sources. The signal bandwidth was then from 0.0064 to 500 Hz . The second group of results in Table I shows that the noise contributed by R_1 and R_2 was lower than that in the former case, in spite of the larger values for the resistors and the lower value of corner frequency in this second case.

Next, we changed both capacitors to 22 nF and used again $R_1 = R_2 = 3.3 \text{ M}\Omega$. By assuming $R_s \ll R_1 + R_2$, the new signal bandwidth was from 0.88 to 500 Hz . The third group of results in Table I shows that the noise contributed by R_1 and R_2 was higher than in the previous case, in spite of the smaller signal bandwidth and the lower value for the resistors in the present case. Further, the noise contributed by R_1 and R_2 and by the noise voltage and noise current for the op-amp was higher than in the first case, in which signal bandwidth was larger.

Finally, we changed R_1 and R_2 to $10 \text{ M}\Omega$ and kept both capacitors at 22 nF . The new signal bandwidth was from 0.29 to 500 Hz . The fourth group of results in Table I shows that some noise sources have a larger contribution and others a lower contribution than in the previous cases. However, Table I also shows that in most cases the noise voltage for the op-amp and the thermal noise caused by R_s are major contributors to the total equivalent input noise. Fig. 3(a) shows the experimental

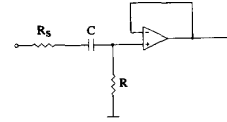


Fig. 4. AC-coupled buffer.

TABLE II
EQUIVALENT INPUT NOISE VOLTAGE (nV, rms) FOR THE DIFFERENT NOISE SOURCES IN FIG. 4 AND FOR DIFFERENT VALUES FOR RESISTORS AND CAPACITORS

	v_1	v_3	v_4	v_5	v_t
$R = 6.6 \text{ M}\Omega$					
$C = 1 \mu\text{F}$					
$R_s = 1 \text{ k}\Omega$	11	91	294	0.09	308
$R_s = 1 \text{ M}\Omega$	972	2498	294	7.8	2700
$R = 20 \text{ M}\Omega$					
$C = 1 \mu\text{F}$					
$R_s = 1 \text{ k}\Omega$	6.5	91	294	0.09	308
$R_s = 1 \text{ M}\Omega$	612	2739	294	8.5	2820

v_1 , v_3 , v_4 , and v_5 , are, respectively, the rms equivalent input noise voltages due to R , R_s , v_n , and i_n . v_t is the total equivalent input noise. The op-amp was an OPA111BM and $T = 300 \text{ K}$.

circuit built to test the results for $R_1 = R_2 = 3.3 \text{ M}\Omega$ and $R_1 = R_2 = 10 \text{ M}\Omega$ when $C_1 = C_2 = 22 \text{ nF}$ and $R_s = 1 \text{ k}\Omega$ in Table I. Fig. 3(b) shows that the input equivalent noise has indeed been reduced when $10 \text{ M}\Omega$ resistors are used as compared to $3.3 \text{ M}\Omega$ resistors. The result was obtained with a Hewlett-Packard 3582A Spectrum Analyzer, using the Hann window, a 300 mHz bandwidth resolution and averaging 128 spectra.

III. NOISE ANALYSIS OF AN AC-COUPLED BUFFER

One of the advantages of the circuit in Fig. 1 is that it does not require large resistors. However, from the previous analysis, it can be seen that the larger the resistors, the lower the output contribution of their thermal noise. It is therefore interesting to consider the noise behavior of an ac-coupled buffer like that in Fig. 4, that requires a large resistor (or capacitor, or both) in order to obtain a very low high-pass frequency.

The corresponding transfer function for the thermal noise associated to R can be obtained from (6) or (7) by letting $R_1 = R$, $R_2 = 0$, $C_1 = 0$, and $C_2 = C$. The result is

$$H(s) = \frac{sR_s C + 1}{s(R + R_s)C + 1}. \quad (13)$$

We find again that, from a given frequency up, the larger the value of R as compared to R_s , the lower the output noise caused by its thermal noise will be.

We have calculated the noise for the circuit in Fig. 4 when $R = 6.6 \text{ M}\Omega$, $C = 1 \mu\text{F}$, the op-amp is an OPA111BM, and the bandwidth for calculating the output noise is from 0.5 to 500 Hz . The signal bandwidth is found to be from 0.024 to 500 Hz . The first group of results in Table II shows that the equivalent input noise for all noise sources and the total noise are lower or equal to those in the first group in Table I, which corresponds to an ac-coupled bootstrap buffer.

$$H_{R_3}(s) = \frac{s^2 R_1 R_2 C_1 C_3 + s[R_1 C_1 + (R_1 + R_2)C_3] + 1}{s^3 R_1 R_2 R_3 C_1 C_2 C_3 + s^2[(R_1 R_2 + R_1 R_3)C_1 C_2 + (R_1 R_3 + R_2 R_3)C_2 C_3] + s[R_1 C_1 + (R_1 + R_2 + R_3)C_2] + 1}. \quad (14)$$

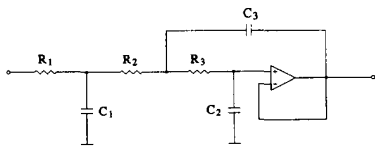


Fig. 5. Voltage-controlled, voltage source (VCVS) ("Sallen-Key") low-pass filter cell with an added first-order stage.

Therefore, we can conclude that although the circuit in Fig. 1 has the advantage of a high ac input impedance, it also has higher noise.

Next, we changed R to 20 M Ω . The signal bandwidth was from 0.008 to 500 Hz. The equivalent input noise for the different noise sources and the total noise for the amplifier are shown as the group of results at the bottom of Table II. We can see that the equivalent noise contributed by R is lower than that in the previous case, in spite of it being more than three times larger than it was before. In addition, the total output noise is only slightly larger than it was in the previous case.

Others [4] have found that for an RC circuit the noise voltage is independent of R . This is because they consider an infinite bandwidth for noise calculations. Here we consider a finite bandwidth from 0.5 to 500 Hz.

IV. NOISE ANALYSIS OF A VOLTAGE-CONTROLLED VOLTAGE SOURCE PROPOSED BY SALLEN AND KEY

Initially, we were at first unaware that the circuit in Fig. 1 had been proposed some time ago by Sallen and Key (it is their circuit number 13 in [5]). We were then curious about whether any of the other circuits which they had proposed had noise behavior similar to that of the circuit in Fig. 1. We were particularly interested in the voltage-controlled voltage source (VCVS) cell, commonly used in low-pass active filters with an added first-order stage (see Fig. 5). The transfer function for the thermal noise voltage associated to R_3 in Fig. 5 when $k = 1$, for example, is as shown in (14) at the bottom of the previous page. The corresponding modulus for this transfer function is shown in Fig. 6. It can be observed that it is very different from the transfer function for the signal, i.e., flat in the pass band and with a 60 dB/decade attenuation in the stop band.

V. CONCLUSION

A larger signal bandwidth and high-value resistors do not necessarily result in an increased equivalent input noise for all circuits. The transfer functions for the different noise sources in a circuit are neither equal among themselves, nor necessarily equal to the transfer function for the signal. Further, the bandwidth for noise calculations is not necessarily the same as the signal bandwidth. This explains why a resistor increase does not always result in an increased equivalent input noise.

However, because of the noise voltage levels of current op-amps, it is not straightforward to experimentally verify the theoretical results for some circuits like that in Fig. 1, which show a paradoxical noise behavior. Nevertheless, it cannot be taken for granted that such a noise behavior is not verifiable in any circuit.

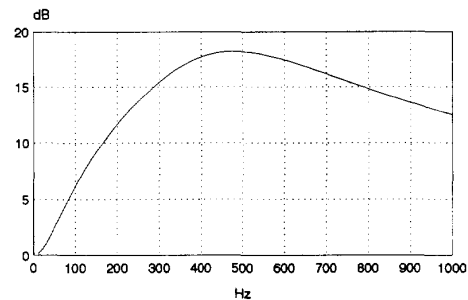


Fig. 6. Magnitude (in decibels) of the transfer function for the noise from resistor R_3 in Fig. 5.

ACKNOWLEDGMENT

The authors are grateful to their colleague Juan Ramos for his help and suggestions during the development of this work.

REFERENCES

- [1] Y. Netzer, "The design of low-noise amplifiers," *Proc. IEEE*, vol. 69, pp. 728-741, June 1981.
- [2] S. Franco, *Design With Operational Amplifiers and Analog Integrated Circuits*. New York: McGraw-Hill, 1988, Section 14.5.
- [3] R. Pallás-Areny, J. Colominas, and J. Rosell, "An improved buffer for bioelectric signals," *IEEE Trans. Biomed. Eng.*, vol. 36, pp. 490-493, Apr. 1989.
- [4] A. B. Carlson, *Communication Systems*, 2nd ed. New York: McGraw-Hill, 1975, Example 3.5.
- [5] R. P. Sallen and E. L. Key, "A practical method of designing RC active filters," *IRE Trans. Circuit Theory*, vol. CT-2, pp. 74-85, Mar. 1955.



Manuel Vargas (S'89-M'93) received the degree of Ingeniero de Telecomunicaci; in 1992 from the Polytechnic University of Catalunya, Barcelona, Spain.

He is Assistant Professor of Electronic Engineering at the same University, where he is working towards the Ph.D. degree. His research interest is high resolution ECG.



Ramón Pallás-Areny (M'81-SM'88) received the Ingeniero Industrial and Doctor Ingeniero Industrial degrees from the Universitat Politècnica de Catalunya, Barcelona, Spain, in 1975 and 1982, respectively.

He is a Professor of Electronic Engineering at the same University, and teaches courses in several areas of medical and electronic instrumentation. His does research on instrumentation methods based on electrical impedance measurements, high resolution ECG and electromagnetic compatibility in electronic systems. He is author of *Basic Electronic Instruments* (1987), *Transducers and Signal Conditioning* (1989) and *Signal Acquisition and Distribution* (1993), coauthor of *An Introduction to Bioengineering* (1988) and of *Electromagnetic Interference in Electronic Systems* (1991), all published in Spanish by Marcombo. He is coauthor with John G. Webster of *Sensors and Signal Conditioning* (Wiley, 1991). In 1989-1990 he was a visiting Fulbright Scholar at the University of Wisconsin-Madison.

He is a member of the Biomedical Engineering Society, The New York Academy of Sciences, and the Instrument Society of America. He was a recipient with John G. Webster of the 1991 Andrew R. Chi Prize Paper Award from the Instrumentation and Measurement Society (IEEE).